

**Title:** Vibrational relaxation and micro-solvation of DF following F-atom reactions in polar solvents

**Authors:** G.T. Dunning<sup>1</sup>, D.R. Glowacki<sup>1,2,2a,2b\*</sup>, T.J. Preston<sup>1</sup>, S.J. Greaves<sup>3</sup>, G.M. Greetham<sup>4</sup>, I.P. Clark<sup>4</sup>, M. Towrie<sup>4</sup>, J.N. Harvey<sup>1</sup> and A.J. Orr-Ewing<sup>1\*</sup>

**Affiliations:**

(1) School of Chemistry, University of Bristol, Cantock's Close, Bristol BS8 1TS, UK.

(2) Department of Computer Science, Merchant Venturers Building, Woodland Road, Bristol BS8 1UB, UK.

(2a) PULSE Institute and Department of Chemistry, Stanford University, Stanford, CA 94305, USA.

(2b) SLAC National Accelerator Laboratory, Menlo Park, California 94025, USA

(3) School of Engineering and Physical Sciences, Heriot-Watt University, Edinburgh, EH14 4AS UK.

(4) Central Laser Facility, Research Complex at Harwell, Science and Technology Facilities Council, Rutherford Appleton Laboratory, Harwell Oxford, Didcot, Oxfordshire, OX11 0QX, UK.

\* Correspondence to:

a.orr-ewing@bristol.ac.uk

+44 1179287672

drglowacki@gmail.com

**One-sentence summary:** Multiple timescales describe the equilibration and solvation of vibrationally excited DF produced from fluorine-atom reactions in polar, deuterated organic solvents.

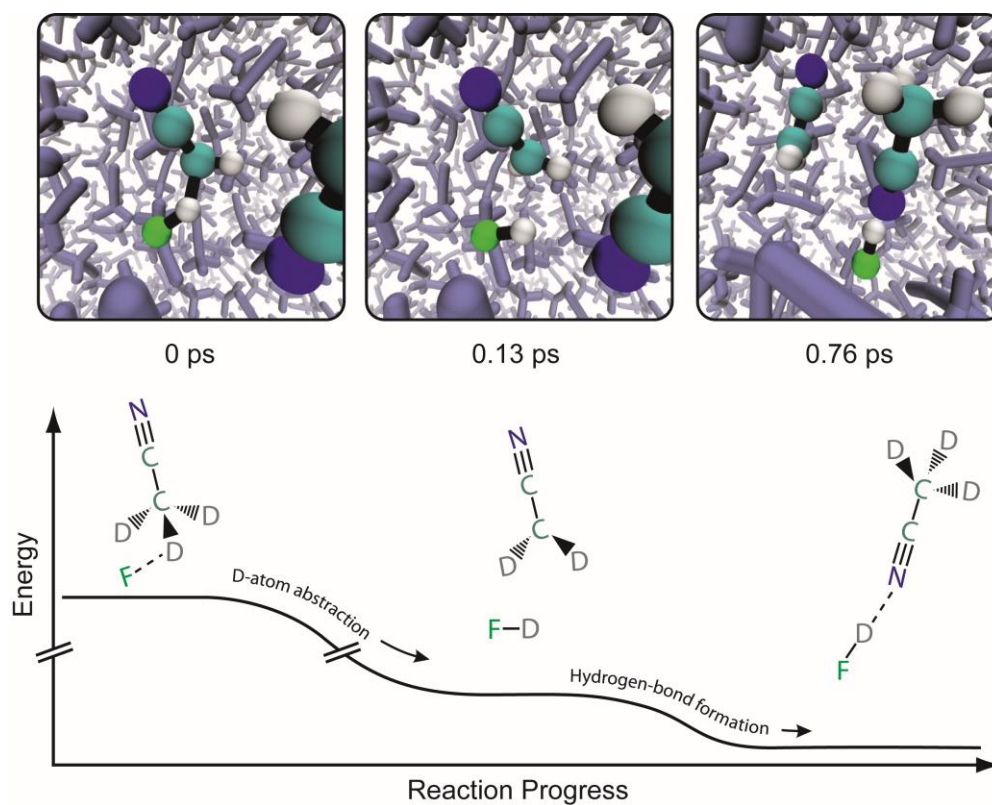
**Abstract:** Solvent-solute interactions influence the mechanisms of chemical reactions in solution, but the response of the solvent is often slower than the reactive event. Here we report that exothermic reactions of F atoms in  $d_3$ -acetonitrile and  $d_2$ -dichloromethane involve efficient energy flow to vibrational motion of the DF product that competes with dissipation of the energy to the solvent bath, despite strong solvent coupling. Transient infrared absorption spectroscopy and molecular dynamics simulations show that after DF forms its first hydrogen bond on a sub-picosecond timescale, DF vibrational relaxation and further solvent restructuring occur over more than 10 ps. Characteristic dynamics of gas-phase F-atom reactions with hydrogen-containing molecules persist in polar organic solvents, and the spectral evolution of the DF products serves as a probe of solvent reorganization induced by a chemical reaction.

**Main text:** Elementary reactions of fluorine atoms are central to the development of our understanding of rates, dynamics and mechanisms of chemical reactions (1, 2). Evidence for rich and subtle dynamical behavior has come from studying hydrogen atom abstractions by F atoms from molecules such as H<sub>2</sub>, H<sub>2</sub>O and CH<sub>4</sub> (or deuterium abstraction from their isotopologues) under isolated-collision conditions in the gas phase. In partnership with quantum-mechanical scattering calculations, sophisticated experiments have probed the transition state (TS) region directly (3, 4), identified non-classical processes that contribute to reaction (5-8), and observed breakdown of the Born-Oppenheimer approximation (9). Early TSs for these exothermic F-atom reactions favor highly vibrationally excited HF or DF molecules (10, 11), consistent with expectations from the Polanyi rules (12). For reactions of F-atoms with hydrocarbons, similar dynamics persist at the gas-liquid interface (13). Here, we extend mechanistic studies of F-atom reactions to the bulk liquid phase and report coupled DF-product and solvent dynamics on the picosecond timescale.

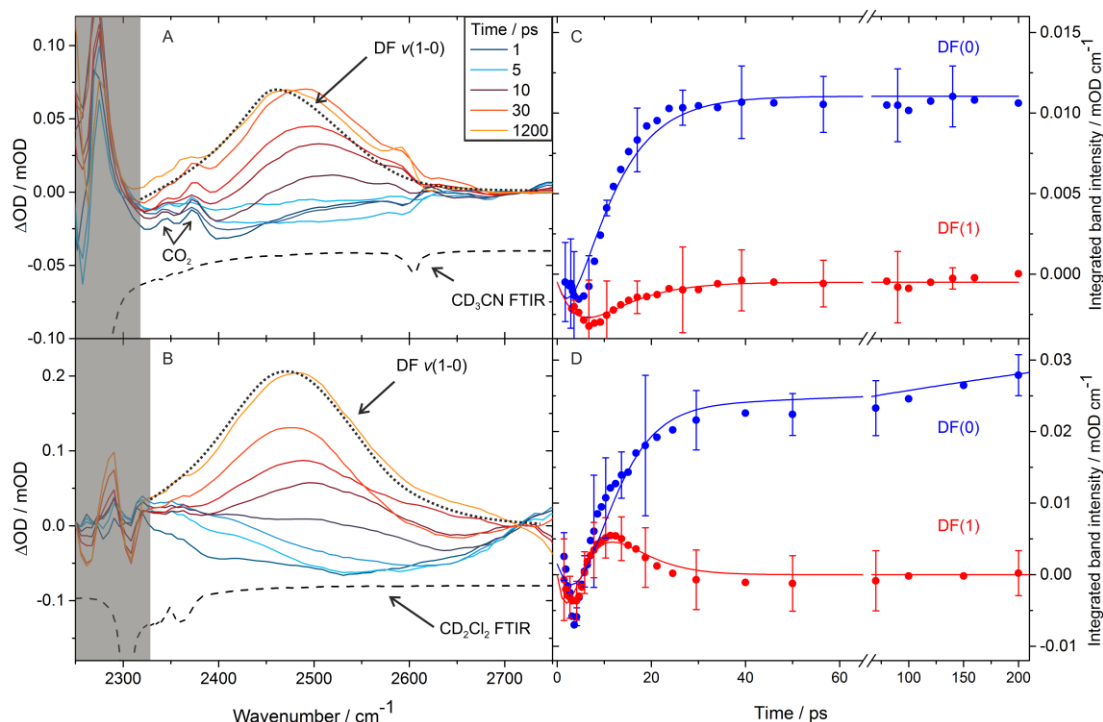
**Bimolecular** chemical reactions in solution are of considerable importance in both chemical synthesis and the biochemistry of living organisms. **Under thermal conditions, these reactions typically occur on the ground state potential energy surface (PES).** The mechanisms of the reactions and the influence of the solvent can be explored using time-resolved spectroscopy and non-equilibrium molecular dynamics (MD) simulations (14-18), **but examples of ultrafast studies of the dynamics of bimolecular reactions of thermalized reagents in liquids remain rare.** The current study shows that exothermic F-atom reactions in CD<sub>3</sub>CN or CD<sub>2</sub>Cl<sub>2</sub> solutions, to produce DF and an organic radical ( $\Delta_r H_0 \approx -150$  kJ mol<sup>-1</sup> (11)), exhibit comparably rich dynamics to their gas phase counterparts, and examines the evolving post-reaction microsolvation environment. **The propensity of nascent DF to hydrogen bond promotes strong solute-solvent coupling, which might be expected to quench the state-specific dynamics. Nevertheless, we observe the formation of highly vibrationally excited DF, with subsequent**

rapid relaxation by energy transfer to the solvent bath. Evidence for a solvent response to the chemical reaction also emerges.

Figure 1 presents frames from an MD simulation that illustrate the early-time dynamics of reaction in  $d_3$ -acetonitrile. Despite reagents which are thermalized, the reaction results in strikingly non-thermal microscopic dynamics in the wake of transition state passage. At the instant of reactive formation, DF molecules have multiple quanta of vibrational excitation, and the surrounding solvent molecules are not oriented to solvate the DF optimally. The solvent environment is thus intermediate between the non-interacting gas-phase limit and the strongly interacting equilibrium limit. Initial hydrogen-bond formation is the first step towards equilibrium solvation of the nascent DF and occurs within a few hundred femtoseconds. Subsequent time-dependent shifts in the DF vibrational frequency over several picoseconds signify both vibrational relaxation and restructuring of the microsolvation environment to accommodate this reaction product.



**Fig. 1:** Snapshots from an MD simulation of an F atom reaction in  $d_3$ -acetonitrile, superimposed on a schematic energy profile. The snapshots show the instant of transition state passage ( $t = 0$  ps), initial separation of  $CD_2CN$  and vibrationally excited  $DF$  ( $t = 0.13$  ps), and reorientation of the  $DF$  and a solvent molecule to establish a hydrogen bond ( $t = 0.76$  ps). Other solvent molecules are shown in gray.



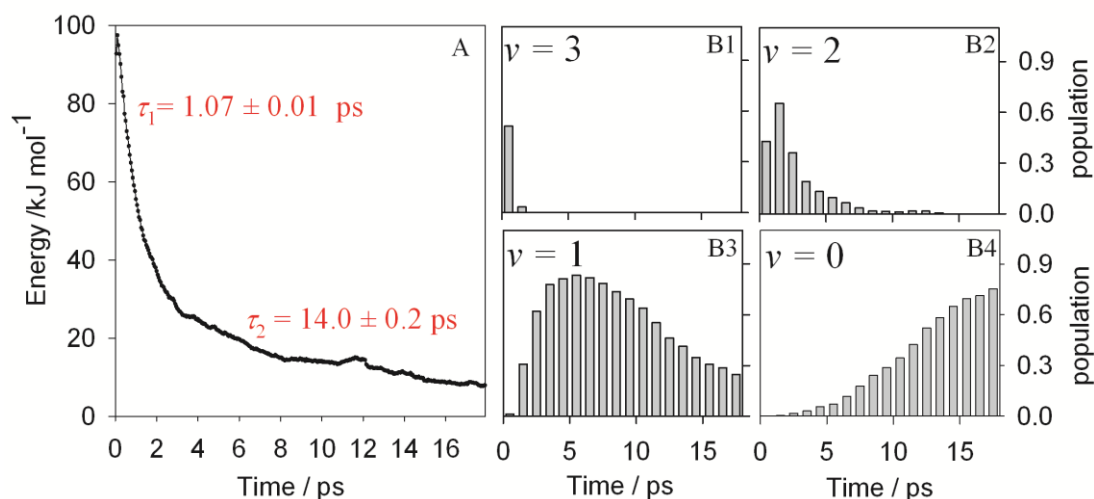
**Fig. 2:** Time-resolved IR absorption spectra and DF band intensities for reactions of F atoms in polar solvents. Panels A, C show results in  $\text{CD}_3\text{CN}$ , B, D in  $\text{CD}_2\text{Cl}_2$ . The inset key shows selected time delays at which the transient spectra were obtained. Negative intensities indicate **stimulated emission because of** vibrational population inversions. The black dotted lines are steady-state FTIR spectra of DF in each solvent, and inverted solvent spectra are shown as dashed lines. Gray shading masks regions of strong solvent absorption. **Decomposition of the spectra into  $v=1 \leftarrow v=0$  and  $v=2 \leftarrow v=1$  bands uses the anharmonicity of the DF vibrational levels, which shifts the  $(2 \leftarrow 1)$  band more than  $100 \text{ cm}^{-1}$  lower than the  $(1 \leftarrow 0)$  band.** The spectral decomposition gives the integrated DF( $v=0$ ) (●) and DF( $v=1$ ) (●) absorption band intensities **shown in panels C and D.** Kinetic fits (solid lines) use a model described in supplementary material (19). Representative error bars are shown for a subset of the data points and are obtained from comparison of fits to 3 data sets.

Figure 2 shows time-resolved infrared (TRIR) absorption spectra of DF following F-atom reactions in CD<sub>3</sub>CN and CD<sub>2</sub>Cl<sub>2</sub>. One-photon photolysis of XeF<sub>2</sub> with 50-fs laser pulses centred at 267 nm promptly generated F atoms in solution (20), and DF products were probed using 50-fs IR laser pulses with >500 cm<sup>-1</sup> bandwidth (19). The broad, unstructured IR bands are characteristic of DF solutes in organic solvents (21). However, the spectral features evolve in time, with a component that moves from lower to higher wavenumber within ~5 ps, and a further shift of ~90 cm<sup>-1</sup> from higher to lower wavenumber over the first 30 ps.

Figure 2 also displays the time-dependent band intensities of the DF( $v=1$  and 0) component absorptions obtained by decomposition of the time-dependent spectra (19). This decomposition makes use of the displacement of the DF ( $v=2 \leftarrow v=1$ ) absorption band by more than 100 cm<sup>-1</sup> to the low wavenumber side of the ( $v=1 \leftarrow v=0$ ) fundamental band because of the large anharmonicity of the DF vibrational levels. The solid lines are the outcomes of fits to a kinetic model in which the F + CD<sub>3</sub>CN or CD<sub>2</sub>Cl<sub>2</sub> reaction produces DF in vibrational levels  $v=2$ , 1 and 0, and vibrational relaxation occurs in single-quantum steps from  $v=2 \rightarrow 1$  and  $v=1 \rightarrow 0$ . The kinetic fits are constrained by data derived from further experiments using UV/visible spectroscopy to monitor the reactive loss of the F-atoms (20) (with time constant  $\tau_F = 4.0 \pm 0.2$  ps in CD<sub>3</sub>CN and  $4.5 \pm 0.8$  ps in CD<sub>2</sub>Cl<sub>2</sub>), and by IR-pump and IR-probe experiments that determined the DF( $v=1 \rightarrow 0$ ) vibrational relaxation time constant in solution ( $\tau_{1 \rightarrow 0} = 3.1 \pm 0.6$  ps in CD<sub>3</sub>CN, compared to  $2.8 \pm 0.3$  ps from our MD simulation) (19). All quoted uncertainties herein correspond to 2 standard deviations (2 SDs).

We concentrate mostly on the outcomes of the F + CD<sub>3</sub>CN reaction, for which both experimental studies and MD simulations were performed. From the fitted rate coefficients obtained from analysis of five independent data sets, we deduce a branching of 55% to DF( $v=2$ ) and 44% to DF( $v=1$ ) products with  $\pm 15\%$  uncertainty and negligible direct production of

DF( $v=0$ ) molecules. Multi-state reactive non-equilibrium atomistic MD simulations of the F + CD<sub>3</sub>CN reaction in a periodic box of 62 fully flexible solvent molecules (19) predict very similar vibrational excitation of DF. Figure 3 illustrates the outcomes of the MD simulations for DF production and relaxation in the immediate wake of the reaction. The computed average energy in vibrational motion of the newly formed DF is almost 100 kJ mol<sup>-1</sup>, and mostly corresponds to DF( $v=2$  and 3). Sub-picosecond relaxation of the DF( $v=3$ ) population is too fast to be resolved experimentally. The vibrational excitation decays through coupling to the solvent bath with two time constants that have a weighted average of  $3.9 \pm 0.18$  ps, in good agreement with the experimentally determined rise of DF( $v=0$ ) absorption.



**Fig. 3:** Transient DF vibrational energy content following D-atom abstractions in *d*<sub>3</sub>-acetonitrile, obtained from the MD simulations. Panel A shows the DF vibrational energy averaged over 200 trajectories with time constants obtained from a bi-exponential fit. Panels B1-B4 show the normalized transient vibrational energy content in the  $v = 0$  to 3 vibrational levels. Exponential fits to the decaying populations of  $v=3$ , 2 and 1 and the rise in  $v = 0$  give time constants of  $\tau_{3 \rightarrow 2} = 0.37 \pm 0.20$  ps,  $\tau_{2 \rightarrow 1} = 3.6 \pm 1.8$  ps and  $\tau_{1 \rightarrow 0} = 6.9 \pm 1.4$  ps.

The negative intensities assigned to DF( $v=1$ ) in Figure 2C indicate **stimulated emission because of** an initially greater population of DF( $v=2$ ). This population inversion is sustained by faster



$v=1 \rightarrow v=0$  than  $v=2 \rightarrow v=1$  relaxation. Strong coupling of the DF vibrational motion to solvent modes facilitates rapid transfer of excess energy to the bath, and the solvent FTIR spectrum (Figure 2) can help identify candidate modes, but cannot predict their quenching ability. The  $v=1 \leftarrow 0$  transition of incompletely solvated DF temporarily overlaps the  $\text{CD}_3\text{CN}$  vibrational mode at  $2600\text{ cm}^{-1}$  enabling efficient energy redistribution. In contrast, the solvent bands below  $2330\text{ cm}^{-1}$  lie more than  $100\text{ cm}^{-1}$  lower than the  $\text{DF}(v=2 \leftarrow 1)$  band center in the early time spectra. The dynamics of F-atom reactions in  $\text{CD}_2\text{Cl}_2$  (Figure 2D) are similar to those observed in  $\text{CD}_3\text{CN}$ , although  $v=2 \rightarrow 1$  relaxation is now found to be faster than  $v=1 \rightarrow 0$ , as expected without resonant coupling to solvent modes. Initial relative populations of  $\text{DF}(v)$  levels are 77% in  $v=2$  and 22% in  $v=1$  ( $\pm 11\%$ ).

We were unable to find a gas-phase study of the  $\text{F} + \text{CD}_3\text{CN}$  reaction with which to compare the liquid-phase  $\text{DF}(v)$  branching. The outcomes of measurements of HF from the  $\text{F} + \text{CH}_3\text{CN}$  reaction in the gas phase instead serve as a benchmark (22), and we deduce lower, but still significant, vibration of the emergent products of reaction in solution despite study in a strongly interacting solvent. For the  $\text{F} + \text{CD}_2\text{Cl}_2$  reaction, direct comparison with gas-phase data also indicates partial solvent quenching of the nascent DF vibrational excitation (11).

Vibrational frequencies are sensitive reporters of the local, dynamic environment of the molecule and provide information on vibrational cooling and solvent restructuring as the system approaches post-reaction equilibrium. Immediately upon formation, DF is vibrationally excited and in an orientation that cannot participate in hydrogen-bonding to the solvent (Figure 1). Different types of non-equilibrium MD simulations help to reveal the microscopic mechanisms at play for short-time relaxation of the nascent DF to equilibrium. The full simulations mimicked the experiments, treating the abstraction and relaxation dynamics, and generated the transient DF spectra shown in Figure 4. Subsequent simulations indicated two

different contributions to DF relaxation in the immediate wake of the abstraction event, as a result of: (i) energy flow from vibrationally excited DF to the solvent; and (ii) changes in the DF microsolvation environment leading to hydrogen bonds. As shown in Figure 4, these two dynamical relaxation processes have opposite effects on the transient DF spectra (19). Relaxation from more energetic vibrational quantum states drives a shift of the DF band to higher wavenumber, as observed experimentally, because of the anharmonicity of the mode. Conversely, reorientation of the DF within its microsolvation environment to form hydrogen-bonded complexes shifts the DF band to lower wavenumber. The MD simulations predict that the latter effect causes a  $220\text{ cm}^{-1}$  shift of the vibrational band center to lower wavenumber, with a time constant  $< 1\text{ ps}$  that accords with prior studies of fast solvation dynamics in acetonitrile (23). This process cannot be followed experimentally because of insufficient build-up of reaction products on this short timescale. However, the computational prediction is consistent with experimental observations of absorption bands below  $2600\text{ cm}^{-1}$  at every time delay, shifted from the  $2907\text{ cm}^{-1}$  fundamental band origin of isolated DF, and also with spectra of  $\text{CD}_3\text{CN}$ —DF complexes (24). The DF subsequently exchanges hydrogen-bonded solvent partners at intervals on the order of  $10\text{ ps}$ .

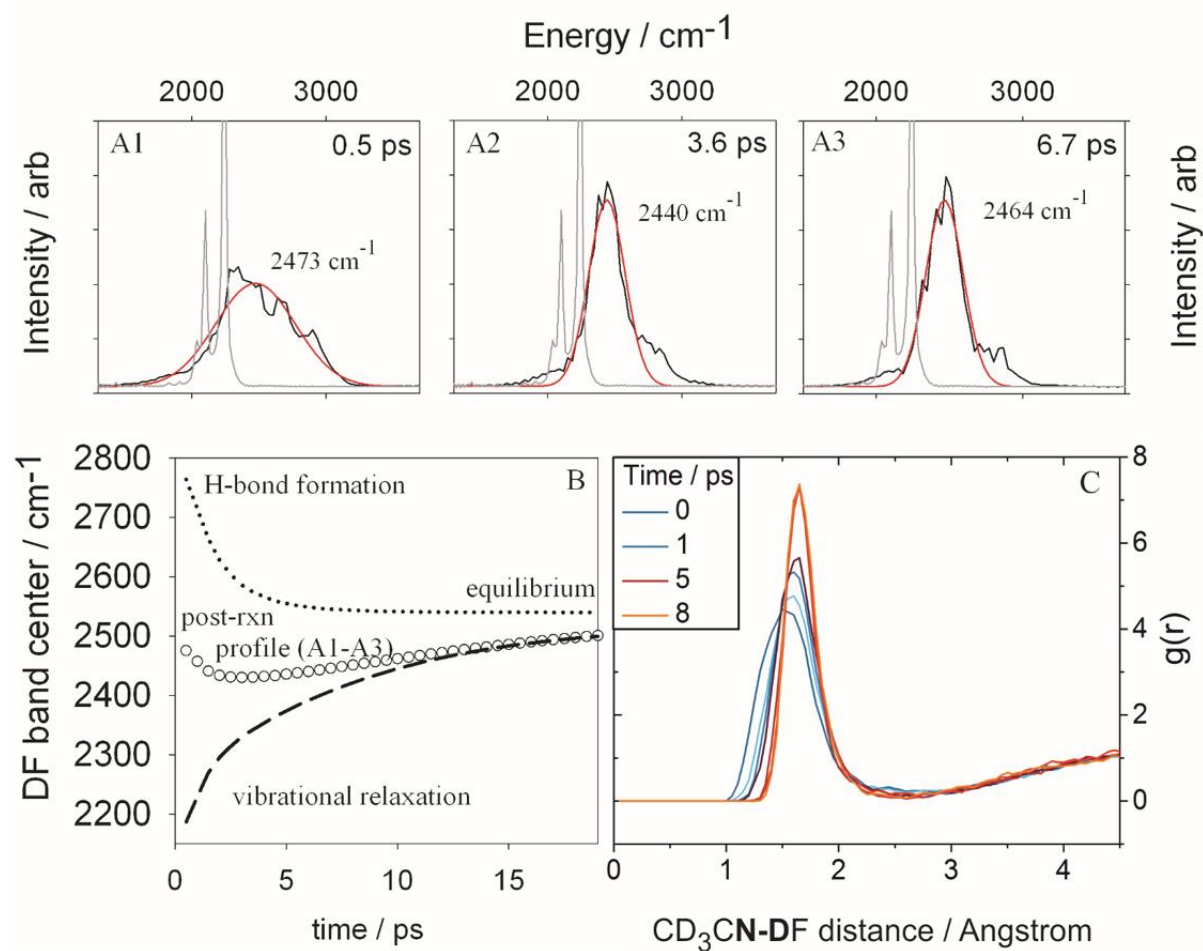


**Fig. 4:** MD simulations of transient power spectra and radial distribution functions. Panel A shows transient DF spectral bands (black lines), Gaussian fits to the simulated DF spectra (red lines), and the simulated solvent spectrum (gray lines). Panel B shows the time-dependent post-reaction profile of the DF band center ( $\circ$ ), together with results from separate simulations that identify spectral effects of hydrogen bond formation with  $\text{CD}_3\text{CN}$  ( $\cdots$ ) and relaxation of vibrationally excited DF ( $---$ ). Panel C shows the time-evolution of the radial distribution function,  $g(r)$ , which describes the changing distribution of distances of the D atom (in DF) to the N-atoms of the  $\text{CD}_3\text{CN}$  solvent molecules.

The time-resolved IR spectra (Figure 2) indicate a second mechanism further contributes to the reduction in DF vibrational wavenumber on a  $\leq 30$  ps timescale. Fits to the experimental spectra incorporate a red shift of the  $\text{DF}(\nu=0 \rightarrow 1$  and  $1 \rightarrow 2)$  absorption bands of  $90 \text{ cm}^{-1}$  with a time constant of 9 to 11 ps (19). MD spectral analysis (e.g. Figure 4 panels A1-A3) reveals a spectral feature to the high wavenumber side of the primary DF band center. This feature arises from DF molecules with a distribution of solvation environments that are not completely relaxed;

solute-solvent hydrogen-bonding is not fully established even at longer times. In qualitative agreement with experimental observations, this peak eventually shifts to lower wavenumber as the DF microsolvation environment approaches equilibrium. We therefore attribute the experimentally observed spectral change to additional restructuring of the solvent around the reaction products, facilitated by hydrogen-bond dynamics (25). The combined experimental and computational outcomes provide the following picture for shifts in the DF fundamental frequency: the initial DF vibrational wavenumber approaches that of an isolated molecule ( $2907\text{ cm}^{-1}$  for DF( $v=0$ )), but incipient H-bonding to a CD<sub>3</sub>CN molecule with time constant  $<1$  ps reduces it by  $\geq 200\text{ cm}^{-1}$ . Further relaxation to the equilibrated  $2480\text{ cm}^{-1}$  band center results from solvent restructuring with time constant  $\approx 10$  ps. These spectral shifts oppose those associated with vibrational cooling of nascent DF( $v>0$ ).

Multiple relaxation timescales have been observed in many solvents (23), and acetonitrile's extensive first- and second-solvent shell structure is consistent with their occurrence here (26). A similar time constant is observed for recovery of the equilibrated DF absorption spectrum when we excite a subset of the DF molecules with an IR laser tuned to be resonant only with the high wavenumber wing of the fundamental band (19). In these latter experiments, the time constant derives solely from changes in the DF solvation environment, but for the reactive results, we cannot rule out solvent restructuring associated with replacement of XeF by one or more CD<sub>3</sub>CN molecules following XeF<sub>2</sub> photolysis (20).

The minimum energy pathway for the reaction of an F atom with a solvent molecule in liquid CD<sub>3</sub>CN is dominated by electronic configurations corresponding to neutral species, with negligible contributions from states deriving from D<sup>+</sup> transfer to the solvent (the  $pK_a$  of HF in acetonitrile is estimated to be  $>20$  (27)). However, at the energies of vibrationally excited DF, our MD simulations demonstrate the transient influence of diabatic states with deuteron-

transfer character on the products' side of the TS. These states are required for an accurate description of the anharmonicity in the solute-solvent coupling, and must be included in our treatment of the reaction PES to give the reported agreement between the MD simulations and experimental measurements of energy disposal to the DF and its subsequent relaxation to the solvent bath.

The current work extends to the liquid phase prior dynamical studies of benchmark fluorine-atom reactions with organic molecules. As we have found in other bimolecular reactions (14, 16), we can apply, with certain caveats, intuition derived from the gas-phase reaction dynamics to the complicated realm of liquids. **Despite strong solute-solvent coupling, the DF products form highly vibrationally excited following reaction in liquid CD<sub>3</sub>CN and CD<sub>2</sub>Cl<sub>2</sub>, but this excitation is lower than for reactions in the gas phase. Solvent damping of the nascent DF vibration may derive from coupling to the energized products as they emerge from the TS and displacement of the TS later along the reaction coordinate.** Equilibration of the excess DF vibrational energy takes 3 to 4 ps in both solvents. Further solvent restructuring to accommodate reaction products continues over **the ensuing** 10 ps. This depth of understanding of a condensed-phase reaction mechanism requires knowledge not only of the PES, but also of the dynamical interplay between solute and solvent. **Vibrational probes of reactions in solution and non-equilibrium MD simulations provide penetrating insights into the dynamics of bond-making and subsequent dissipation of excess chemical energy to the solvent. Further exploration using this combined methodology will provide increasingly detailed descriptions of the effect of emergent product vibrational excitation on reaction outcomes in complex systems.**

## References and Notes:

1. R. D. Levine, *Molecular Reaction Dynamics*. (Cambridge University Press, Cambridge, 2005).
2. D. M. Neumark, A. M. Wodtke, G. N. Robinson, C. C. Hayden, Y. T. Lee, Molecular-Beam Studies of the F+H<sub>2</sub> Reaction. *J Chem Phys* **82**, 3045-3066 (1985).
3. W. R. Dong, C. L. Xiao, T. Wang, D. X. Dai, X. M. Yang, D. H. Zhang, Transition-State Spectroscopy of Partial Wave Resonances in the F plus HD Reaction. *Science* **327**, 1501-1502 (2010).
4. D. E. Manolopoulos, K. Stark, H. J. Werner, D. W. Arnold, S. E. Bradforth, D. M. Neumark, The Transition-State of the F+H<sub>2</sub> Reaction. *Science* **262**, 1852-1855 (1993).
5. M. Tizniti, S. D. Le Picard, F. Lique, C. Berteloite, A. Canosa, M. H. Alexander, I. R. Sims, The rate of the F + H<sub>2</sub> reaction at very low temperatures. *Nat Chem* **6**, 141-145 (2014).
6. M. H. Qiu, Z. F. Ren, L. Che, D. X. Dai, S. A. Harich, X. Y. Wang, X. M. Yang, C. X. Xu, D. Q. Xie, M. Gustafsson, R. T. Skodje, Z. G. Sun, D. H. Zhang, Observation of Feshbach resonances in the F+H<sub>2</sub> → HF+H reaction. *Science* **311**, 1440-1443 (2006).
7. T. Wang, J. Chen, T. G. Yang, C. L. Xiao, Z. G. Sun, L. Huang, D. X. Dai, X. M. Yang, D. H. Zhang, Dynamical Resonances Accessible Only by Reagent Vibrational Excitation in the F + HD → HF + D Reaction. *Science* **342**, 1499-1502 (2013).
8. R. Otto, J. Y. Ma, A. W. Ray, J. S. Daluz, J. Li, H. Guo, R. E. Continetti, Imaging Dynamics on the F + H<sub>2</sub>O → HF + OH Potential Energy Surfaces from Wells to Barriers. *Science* **343**, 396-399 (2014).
9. L. Che, Z. F. Ren, X. G. Wang, W. R. Dong, D. X. Dai, X. Y. Wang, D. H. Zhang, X. M. Yang, L. S. Sheng, G. L. Li, H. J. Werner, F. Lique, M. H. Alexander, Breakdown of the Born-Oppenheimer approximation in the F+o-D<sub>2</sub> → DF+D reaction. *Science* **317**, 1061-1064 (2007).
10. J. J. Lin, J. G. Zhou, W. C. Shiu, K. P. Liu, State-specific correlation of coincident product pairs in the F+CD<sub>4</sub> reaction. *Science* **300**, 966-969 (2003).
11. M. A. Wickramaratne, D. W. Setser, H. Hildebrandt, B. Korbitzer, H. Heydtmann, Evaluation of HF Product Distributions Deduced from Infrared Chemiluminescence .2. F-Atom Reactions. *Chem Phys* **94**, 109-129 (1985).
12. J. C. Polanyi, Concepts in reaction dynamics. *Acc. Chem. Res.* **5**, 161-168 (1972).
13. A. M. Zolot, P. J. Dagdigan, D. J. Nesbitt, Quantum-state resolved reactive scattering at the gas-liquid interface: F + squalane (C<sub>30</sub>H<sub>62</sub>) dynamics via high-resolution infrared absorption of nascent HF(v,J). *J. Chem. Phys.* **129**, 194705 (2008).
14. S. J. Greaves, R. A. Rose, T. A. A. Oliver, D. R. Glowacki, M. N. R. Ashfold, J. N. Harvey, I. P. Clark, G. M. Greetham, A. W. Parker, M. Towrie, A. J. Orr-Ewing, Vibrationally Quantum-State-Specific Reaction Dynamics of H Atom Abstraction by CN Radical in Solution. *Science* **331**, 1423-1426 (2011); published online Epub March 18, 2011 (10.1126/science.1197796).
15. R. A. Rose, S. J. Greaves, T. A. A. Oliver, I. P. Clark, G. M. Greetham, A. W. Parker, M. Towrie, A. J. Orr-Ewing, Vibrationally quantum-state-specific dynamics of the reactions of CN radicals with organic molecules in solution. *J. Chem. Phys.* **134**, 244503 (2011).
16. A. J. Orr-Ewing, Perspective: Bimolecular chemical reaction dynamics in liquids. *J Chem Phys* **140**, 090901 (2014).

17. D. R. Glowacki, A. J. Orr-Ewing, J. N. Harvey, Product energy deposition of CN + alkane H abstraction reactions in gas and solution phases. *J. Chem. Phys.* **134**, 214508-214511 (2011).
18. D. R. Glowacki, R. A. Rose, S. J. Greaves, A. J. Orr-Ewing, J. N. Harvey, Ultrafast energy flow in the wake of solution-phase bimolecular reactions. *Nature Chem.* **3**, 850-855 (2011).
19. Materials and methods are available as supporting material on Science Online.
20. G. T. Dunning, T. J. Preston, A. J. Orr-Ewing, S. J. Greaves, G. M. Greetham, I. P. Clark, M. Towrie, Dynamics of photodissociation of XeF<sub>2</sub> in organic solvents *Phys. Chem. Chem. Phys.* **16**, 16095 - 16102 (2014).
21. R. M. Adams, J. J. Katz, Infrared Spectral Studies of Hydrogen Bonding Phenomena in Solutions Containing Hydrogen Fluoride. *J. Mol. Spectrosc.* **1**, 306-332 (1957).
22. K. Dehe, H. Heydtmann, HF infrared emission from the reactions of atomic fluorine with methylcyanide, methylisocyanide, dimethylsulfide and dimethyldisulfide. *Chem Phys Lett* **262**, 683-688 (1996).
23. B. Bagchi, B. Jana, Solvation dynamics in dipolar liquids. *Chem. Soc. Rev.* **39**, 1936-1954 (2010).
24. G. L. Johnson, L. Andrews, Infrared-Spectra of Hydrogen-Bonded Complexes between CH<sub>3</sub>CN and HF in Solid Argon at 12-K. *J. Phys. Chem.* **87**, 1852-1859 (1983).
25. R. Rey, K. B. Moller, J. T. Hynes, Hydrogen bond dynamics in water and ultrafast infrared spectroscopy. *J. Phys. Chem. A* **106**, 11993-11996 (2002).
26. W. L. Jorgensen, J. M. Briggs, Monte-Carlo Simulations of Liquid Acetonitrile with a 3-Site Model. *Mol. Phys.* **63**, 547-558 (1988).
27. C. R. Nicoleti, V. G. Marini, L. M. Zimmermann, V. G. Machado, Anionic Chromogenic Chemosensors Highly Selective for Fluoride or Cyanide Based on 4-(4-Nitrobenzylideneamine)phenol. *J. Brazil Chem. Soc.* **23**, 1488-1500 (2012).
28. G. M. Greetham, P. Burgos, Q. Cao, I. P. Clark, P. S. Codd, R. C. Farrow, M. W. George, M. Kogimtzis, P. Matousek, A. W. Parker, M. R. Pollard, D. A. Robinson, Z.-J. Xin, M. Towrie, ULTRA: A Unique Instrument for Time-Resolved Spectroscopy *Appl. Spectrosc.* **64**, 1311-1319 (2010).
29. G. Black, R. L. Sharpless, D. C. Lorents, D. L. Huestis, R. A. Gutcheck, T. D. Bonifield, D. A. Helms, G. K. Walters, XeF<sub>2</sub> Photo-Dissociation Studies .1. Quantum Yields and Kinetics of XeF(B) and XeF(C). *J. Chem. Phys.* **75**, 4840-4846 (1981).
30. M. P. Grubb, A. J. Orr-Ewing, M. N. R. Ashfold, KOALA: a program for the processing and decomposition of transient spectra. *Rev. Sci. Instrumen.* **86**, 064104 (2014).
31. M. M. Shaw, R. G. Smith, C. A. Ramsden, F-19 NMR and UV studies of xenon difluoride solution-vessel stability and its relevance to the fluorination of organic substrates. *Arkivoc*, 221-U976 (2011).
32. F. Abou-Chahine, T. J. Preston, G. T. Dunning, A. J. Orr-Ewing, G. M. Greetham, I. P. Clark, M. Towrie, S. A. Reid, Photo-isomerization and photo-induced reactions in liquid CCl<sub>4</sub> and CHCl<sub>3</sub>. *J. Phys. Chem. A* **117**, 13388-13398 (2013).
33. G. Bucher, J. C. Scaiano, Absolute rate constants for atomic fluorine in solution - characterization of reaction intermediates in the laser flash-photolysis of xenon difluoride. *J. Am. Chem. Soc.* **116**, 10076-10079 (1994).
34. G. LeBras, N. I. Butkovskaya, I. I. Morozov, V. L. Talrose, Reaction of F-Atoms with Dichloromethane by Modulated Molecular-Beam Mass-Spectrometry. *Chem. Phys.* **50**, 63-69 (1980).
35. NIST Webbook, *National Institute of Standards and Technology*, P. J. Linstrom, W. G. Mallard, Eds. (Gaithersburg MD, 20899).

36. L. Andrews, G. L. Johnson, FTIR Spectra of Water Hydrogen-Fluoride Complexes in Solid Argon - Evidence for Inversion Doubling in the HF Librational Modes of H<sub>2</sub>O-HF. *J. Chem. Phys.* **79**, 3670-3677 (1983).
37. N. I. Sushko, V. F. Sukhoverkhov, E. G. Tarakanova, G. V. Yuxhnevich, The IR spectra of solutions of hydrogen fluoride in (CH<sub>3</sub>)<sub>2</sub>NCHO, (CH<sub>3</sub>)<sub>2</sub>CO, and CH<sub>3</sub>CN with a molar ratio of the components of 0 : 1-10 : 1. *J. Opt. Technol.* **73**, 515-518 (2006).
38. G. V. Yuxhnevich, E. G. Tarakanova, IR spectroscopic analysis of the composition of heterocomplexes formed in a binary system. *Opt. Spectrosc.* **101**, 708-715 (2006).
39. R. A. Nicodemus, S. A. Corcelli, J. L. Skinner, A. Tokmakoff, Collective Hydrogen Bond Reorganization in Water Studied with Temperature-Dependent Ultrafast Infrared Spectroscopy. *J. Phys. Chem. B* **115**, 5604-5616 (2011).
40. H. J. Werner, G. Knizia, F. R. Manby, Explicitly correlated coupled cluster methods with pair-specific geminals. *Mol. Phys.* **109**, 407-417 (2011).
41. A. Warshel, R. M. Weiss, An Empirical Valence Bond Approach for Comparing Reactions in Solutions and in Enzymes. *J. Am. Chem. Soc.* **102**, 6218-6226 (1980).
42. T. A. Halgren, Merck molecular force field .1. Basis, form, scope, parameterization, and performance of MMFF94. *J. Comput. Chem.* **17**, 490-519 (1996).
43. B. R. Brooks, C. L. Brooks, A. D. Mackerell, L. Nilsson, R. J. Petrella, B. Roux, Y. Won, G. Archontis, C. Bartels, S. Boresch, A. Caflisch, L. Caves, Q. Cui, A. R. Dinner, M. Feig, S. Fischer, J. Gao, M. Hodoscek, W. Im, K. Kuczera, T. Lazaridis, J. Ma, V. Ovchinnikov, E. Paci, R. W. Pastor, C. B. Post, J. Z. Pu, M. Schaefer, B. Tidor, R. M. Venable, H. L. Woodcock, X. Wu, W. Yang, D. M. York, M. Karplus, CHARMM: The Biomolecular Simulation Program. *J. Comput. Chem.* **30**, 1545-1614 (2009).
44. D. R. Glowacki, A. J. Orr-Ewing, J. N. Harvey, A Parallel Multistate Framework for Atomistic Non-Equilibrium Reaction Dynamics of Solutes in Strongly Interacting Organic Solvents: F Abstraction Reactions in d-Acetonitrile. ArXiv 1412.4180 (2014).
45. R. A. Rose, S. J. Greaves, F. Abou-Chahine, D. R. Glowacki, T. A. A. Oliver, M. N. R. Ashfold, I. P. Clark, G. M. Greetham, M. Towrie, A. J. Orr-Ewing, Reaction dynamics of CN radicals with tetrahydrofuran in liquid solutions. *Phys. Chem. Chem. Phys.* **14**, 10424-10437 (2012).
46. D. R. Glowacki, S. K. Reed, M. J. Pilling, D. V. Shalashilin, E. Martinez-Nunez, Classical, quantum and statistical simulations of vibrationally excited HOSO<sub>2</sub>: IVR, dissociation, and implications for OH + SO<sub>2</sub> kinetics at high pressures. *Phys. Chem. Chem. Phys.* **11**, 963-974 (2009).
47. D. R. Glowacki, E. Paci, D. V. Shalashilin, Boxed Molecular Dynamics: A Simple and General Technique for Accelerating Rare Event Kinetics and Mapping Free Energy in Large Molecular Systems. *J. Phys. Chem. B* **113**, 16603-16611 (2009).
48. D. R. Glowacki, E. Paci, D. V. Shalashilin, Boxed Molecular Dynamics: Decorrelation Time Scales and the Kinetic Master Equation. *J. Chem. Theory Comput.* **7**, 1244-1252 (2011).
49. G. A. Voth, Computer simulation of proton solvation and transport in aqueous and biomolecular systems. *Accounts Chem. Res.* **39**, 143-150 (2006).
50. M. L. Horng, J. A. Gardecki, A. Papazyan, M. Maroncelli, Subpicosecond Measurements of Polar Solvation Dynamics - Coumarin-153 Revisited. *J. Phys. Chem.* **99**, 17311-17337 (1995).
51. S. J. Rosenthal, X. L. Xie, M. Du, G. R. Fleming, Femtosecond Solvation Dynamics in Acetonitrile - Observation of the Inertial Contribution to the Solvent Response. *J. Chem. Phys.* **95**, 4715-4718 (1991).



**Acknowledgements:** The Bristol group thanks the Engineering and Physical Sciences Research Council (EPSRC, Programme Grant EP/G00224X and a studentship for GTD) and the European Research Council (ERC, Advanced Grant 290966 CAPRI) for financial support. DRG acknowledges award of a Royal Society University Research fellowship, JNH acknowledges a Royal Society Wolfson Merit Award, and SJG thanks EPSRC for award of a Career Acceleration Fellowship (EPSRC EP/J002534/2). Experimental measurements were conducted at the ULTRA Laser Facility which is supported by the Science and Technology Facilities Council (STFC, Facility Grant ST/501784). We are grateful to F. Abou-Chahine for assistance with collection of some of the experimental data, and to M.P. Grubb and M.N.R. Ashfold for valuable discussions.

All experimental data and analysis files are archived in the University of Bristol's Research Data Storage Facility. Supplementary Materials contains summaries of the data analysis procedures and outcomes.

**Individual contributions to the work:** AJOE and GTD devised and carried out the experiments, with assistance from SJG, and analysed the experimental data with TJP and SJG. GMG, IPC and MT constructed and operated the ultrafast laser system at the Central Laser Facility with which all experimental data were collected. DRG and JNH devised and performed the MD simulations and analysed the computational results. AJOE, GTD, TJP, DRG and JNH wrote the paper.

## **Supplementary Materials**

Materials and methods

Figs. S1 to S7

Tables S1 to S2

References (28-51)